International Journal of Geo-Information

MDPI

Article

Classification of Floods in Europe and North America with Focus on Compound Events

Steven Brazda [1,2], Mojca Šraj [2] and Nejc Bezak [2,*]

[1] BGC Engineering Inc., Vancouver, BC V6Z 0C8, Canada
[2] Faculty of Civil and Geodetic Engineering, University of Ljubljana, 1000 Ljubljana, Slovenia
* Correspondence: nejc.bezak@fgg.uni-lj.si

Abstract: Compound events occur when multiple drivers or hazards occur in the same region or on the same time scale, hence amplifying their impacts. Compound events can cause large economic damage or endanger human lives. Thus, a better understanding of the characteristics of these events is needed in order to protect human lives. This study investigates the drivers and characteristics of floods in Europe and North America from the compound event perspective. More than 100 catchments across Europe and North America were selected as case study examples in order to investigate characteristics of floods during a 1979–2019 period. Air temperature, precipitation, snow thickness, snow liquid water equivalent, wind speed, vapour pressure, and soil moisture content were used as potential drivers. Annual maximum floods were classified into several flood types. Predefined flood types were snowmelt floods, rain-on-snow floods, short precipitation floods and long precipitation floods that were further classified into two sub-categories (i.e., wet and dry initial conditions). The results of this study show that snowmelt floods were often the dominant flood type in the selected catchments, especially at higher latitudes. Moreover, snow-related floods were slightly less frequent for high altitude catchments compared to low- and medium-elevation catchments. These high-altitude areas often experience intense summer rainstorms that generate the highest annual discharges. On the other hand, snowmelt-driven floods were the predominant flood type for the lower elevation catchments. Moreover, wet initial conditions were more frequent than the dry initial conditions, indicating the importance of the soil moisture for flood generation. Hence, these findings can be used for flood risk management and modelling.

Keywords: floods; compound events; flood typologies; precipitation; catchment characteristics

Citation: Brazda, S.; Šraj, M.; Bezak, N. Classification of Floods in Europe and North America with Focus on Compound Events. *ISPRS Int. J. Geo-Inf.* **2022**, *11*, 580. https://doi.org/10.3390/ijgi11120580

Academic Editor: Wolfgang Kainz

Received: 6 September 2022
Accepted: 20 November 2022
Published: 22 November 2022

1. Introduction

Floods are a natural hazard that can cause large economic damage and endanger human lives [1–3]. In order to protect human lives and property, either effective early warning systems or comprehensive flood-risk management are needed. In order to implement flood risk management measures such as hybrid flood protection infrastructure, understanding of flood mechanisms across different spatial scales, climates, elevations and other catchment-related characteristics is required [1]. This also applies to the snowmelt-related floods [2,3], which are the focus of this study.

Snow cover and snowmelt can affect the occurrence of floods in different ways. For example, a combination of snowmelt and intense precipitation with higher air temperature can generate so-called rain-on-snow floods, which can cause significant flood damage due to the compound effect. In recent years, special attention has been given to various compound events. Definitions and typologies for compound events were recently presented by Zscheischler et al. (2020) [1]. According to Zscheischler et al. (2020) [1], compound events can be classified into four main types, namely preconditioned events, multivariate events, temporally compounding events and spatially compounding events. Preconditioned events are hazards created or exacerbated by a pre-existing condition, as in the case of rain-on-snow

floods [2,3]. Multivariate events are caused by multiple drivers and/or hazards occurring in the same geographic region within a temporal boundary, such as a combination of fluvial and coastal floods or a combination of drought and heat waves [4,5]. Temporally compounding events are a sequence of hazards occurring in a spatially bounded region, such as a series of large rainstorms causing flooding [6–8]. Spatially compounding events experience single or multiple hazards within a given time period [9,10], such as the large floods that occurred in Germany, Belgium and the Netherlands in 2021 [11].

This study focuses on compound events, where snowmelt is one of the driving forces of flooding. These type of events occur most frequently in northern regions in the northern hemisphere and conversely in the southern hemisphere, and in alpine areas [3,12,13]. This type of hazard becomes a potential threat for society when snow depth increases during the winter and then melts rapidly as a result of a sudden temperature rise or precipitation event. The significant melting of snow can saturate the soil and consequently lead to excessive surface runoff that can cause flooding, especially in cases when the ground is frozen. Many rivers around the globe experience this type of flooding each year. If it rains at the same time as the snow melts, even more severe flooding can occur, known as rain-on-snow floods [2,3]. Not many studies have been conducted that focus on examining the characteristics of rain-on-snow floods at large spatial scales. Most studies have been conducted focusing on smaller spatial scales. For example, Sikorska et al. (2015) [14] classified the most frequent flood types in Switzerland into six categories: snowmelt, rain-on-snow, flash, glacier-melt, short-rainfall and long-rainfall floods. Floods were classified using decision tree and the fuzzy method [14]. This study demonstrated that the predominant flood types in Switzerland are long-rainfall and short-rainfall floods. The potential drivers of flood events were also examined by Merz and Blöschl (2003) [15], who investigated floods in Austria. They found that there are significant regional differences between different climatic and terrain zones in Austria. Furthermore, they also analyzed the seasonality of flooding, which indicates the time of the year when the catchments are most likely to be flooded. Additionally, the authors reported that long-term rainfall events are the main cause of flooding in Austria. Recently, Berghuijs et al. (2019) [16] examined the potential drivers of the most extreme floods across Europe. The main drivers considered were snowmelt, extreme precipitation, and high antecedent soil moisture. Extreme precipitation (i.e., maximum annual discharge is a result of the largest precipitation event) was found to be the least dominant driver in generating floods in Europe. On the other hand, this mechanism was the most pronounced in the mountainous regions of the Alps and the Carpathians. Furthermore, the melting of snow was the second-most important flood generation mechanism in Europe, with this factor dominating in Eastern Europe and Scandinavia. However, [16] showed that the most important flood generation mechanism across Europe was high antecedent moisture. It should be noted that [16] focused primarily on the flood dates and did not consider the complete flood hydrographs.

There are still many open questions that need to be addressed to improve the understanding and prediction of floods, e.g., the seasonal characteristics of snow-related events, which climate factors are the main drivers of floods, etc. Therefore, the main aim of this paper is to classify floods into different categories according to their causes and to identify which flood types are most common in different parts of Europe and North America. Additionally, this study also focuses on analyzing the relationships between flood types and elevation, climate zone, and catchment area.

2. Data

The research includes 107 catchments throughout Europe and North America. The selected catchments are shown in Figures 1 and 2 for North America and Europe, respectively. A detailed list of selected catchments with their main characteristics is presented in the Supplement prepared (Table S1) based on Brazda (2021) [17]. These 107 catchments were manually selected to include catchments in different climate zones, elevations, etc., and with the most complete discharge dataset. The focus of this study was Europe and North

America and catchments located between 40° and 70° latitude were selected. Hence, all these catchments are located in the mid-latitudes, meaning that all four seasons (autumn, winter, spring, summer) define the climate characteristics. Additionally, nested catchments were not taken into consideration. Hence, the idea was to have roughly uniform distribution of catchments in these two continents based on the above limitations and discharge data availability. For all catchments, the AM sample was visually checked in order to detect possible significant changes in the sample size due to human impact (e.g., dam construction). We argue that these 107 catchments are a valid representation of a typical catchment for the selected study area.

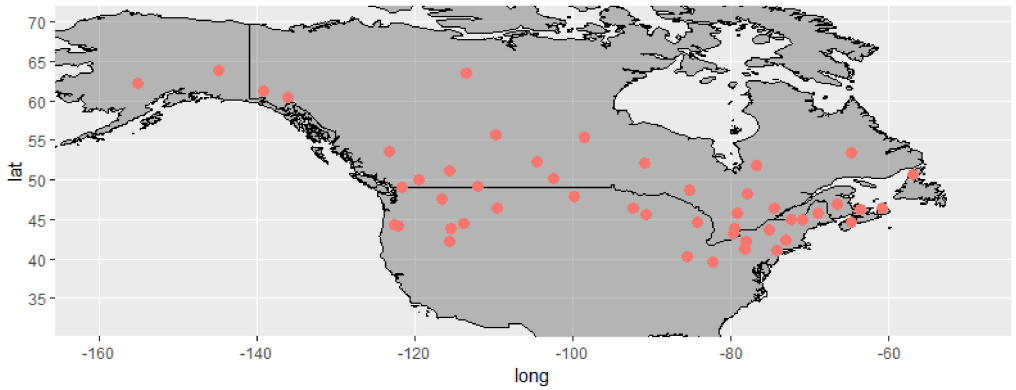

Figure 1. Gauging stations locations for catchments that were selected in North America.

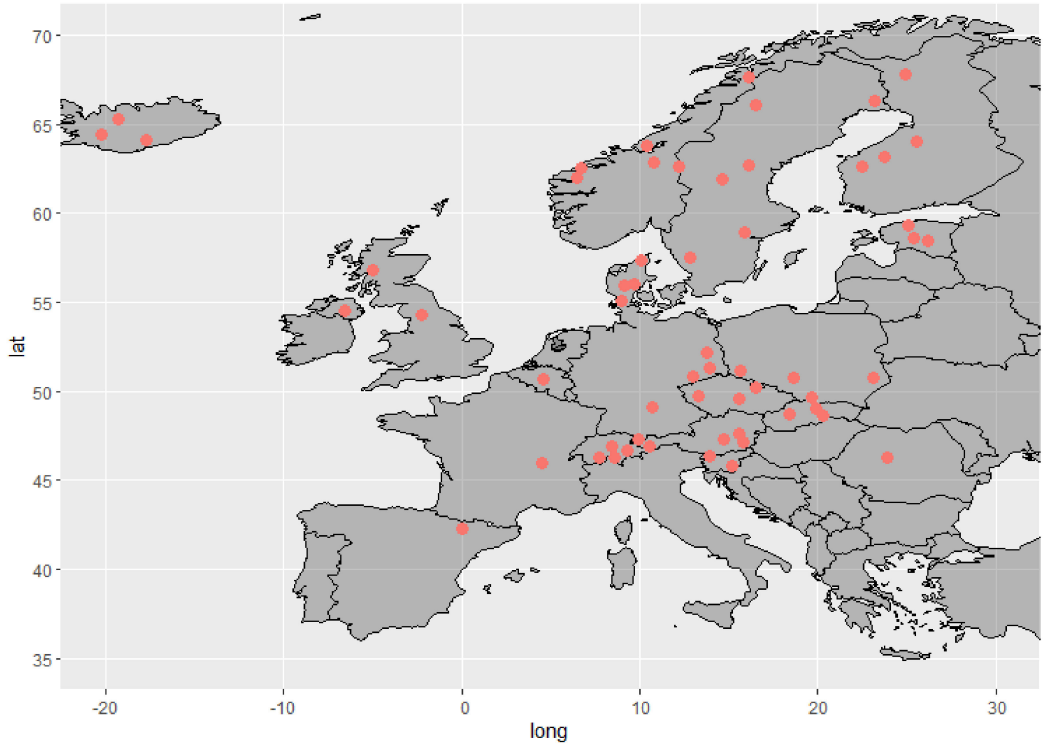

Figure 2. Gauging stations locations for catchments that were selected in Europe.

Daily discharge data for the selected catchments were obtained from the Global Runoff Data Centre [18]. Daily mean discharge from 1979 to 2019 was used in the study. Additionally, the catchment boundaries were also obtained from the GRDC [18]. Figure 3 shows an example of the daily discharge time series for the Penobscot River catchment in the USA, which was one of the selected catchments in North America.

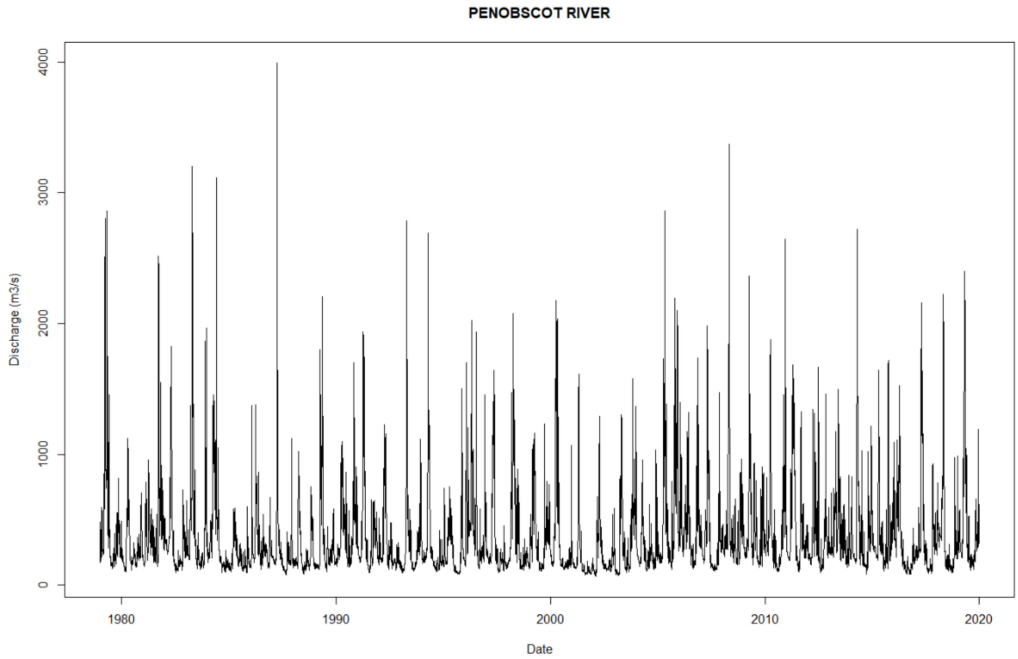

Figure 3. Example of the river discharge time series for one of the investigated catchments for the period 1979–2019. River discharge data were obtained from the GRDC. The Penobscot river is located in the USA and has a catchment area of 17,317 km^2, and most of the catchment area is located in the Warm Summer Humid Continental climate zone.

The Köppen–Geiger system [19] was used to identify the corresponding climate zone of each of the selected catchments. The Climate Change and Infectious Diseases Group [19] was used to obtain the climate zone data. Table 1 shows the climate zones that were considered. The distribution of catchments per climate zone is shown in the Supplement (Figure S1).

Table 1. The climate zones of the considered catchments based on the Köppen–Geiger system.

Acronym	Climate Zone
BSK	Cold Semi-Arid
CFA	Humid Subtropical
CFB	Temperate Oceanic
CFC	Subpolar Oceanic
CSB	Warm Summer Mediterranean
DFA	Hot Summer Humid Continental
DFB	Warm Summer Humid Continental
DFC	Subarctic
DSB	Mediterranean-Influenced Warm Summer Humid Continental
DSC	Mediterranean-Influenced Subarctic
ET	Tundra

Global elevation data were downloaded from EarthEnv [20] to determine the catchment mean elevation. The elevation data used in this study were a gridded dataset with a spatial resolution of 1 km. Figure 4 shows the elevation data and the catchment boundaries. The distribution of catchments per elevation zone is shown in the Supplement (Figure S3).

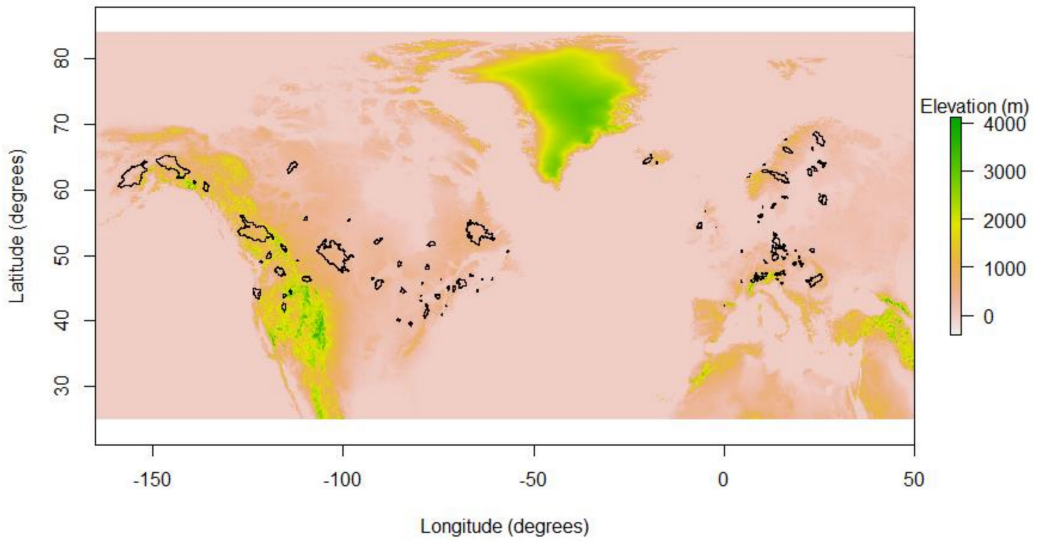

Figure 4. The elevation (m.a.s.l.) data with catchment boundaries (black polygons).

All climate data, except soil moisture data, were obtained from the Copernicus Agrometeorological Indicators Data Store [21]. The period used was 1979–2019. The grids had a spatial resolution of 0.1°. Table 2 displays all the climate information downloaded and used in the scope of this study.

Table 2. List of climate variables that were taken into consideration in the scope of this study.

Variable	Description	Unit
Temperature	Mean 24 h air temperature at a 2 m height	K
Precipitation	Total volume of water fallen per unit area over the 24 h period	mm/day
Snow Thickness	Mean depth of snow cover over the 24 h period	cm
Snow Thickness Liquid Water Equivalent (LWE)	Mean depth of liquid over the 24 h period assuming all snow melts and there is no runoff, soil penetration or evaporation	cm
Vapour Pressure	Mean water vapour pressure measured over the 24 h period	hPa
Wind Speed	Mean wind speed at 10 m height	m/s
Soil Moisture	Volume of water in the top soil layer (0–7 cm depth)	m^3/m^3

Soil moisture data were obtained from the Copernicus Data Store [22]. Hourly ERA5 data at individual levels from 1979 to the present was used. The hourly value at 12:00 was used for further analysis. ERA5 is one of the products that is frequently used in many different fields [4,23–25], providing a reanalysis of global climate and weather that combines model data with observations into a globally complete and consistent dataset using data assimilation technique.

3. Methods

3.1. Flood Hydrograph Seperation

R software was used to conduct the data analysis (i.e., data import, clipping of the gridded data, etc.) [26]. The Annual Maximum (AM) method [27–30] was used to determine the flood events. In the scope of this study, we did not focus only on peak discharge values but we extracted the entire flood hydrographs [29], which was not the case in some previous studies [16]. We decided to extract the climate data for the entire duration of the hydrograph rather than just extracting data only on the day of the maximum peak discharge. This is because in many catchments there is a lag between precipitation and runoff, and the flood-driving climate factors often occur on the days before the peak. Baseflow separation

was used to determine the start and the end of the hydrograph. It is a frequently used method for hydrograph definition [29,31,32]. Baseflow is often considered as part of the stream water that originates from groundwater [32]. The surface runoff hydrograph starts when overland flow exceeds baseflow and ends when there is no more water belonging to the overland runoff. To determine the shape of the hydrograph, as well as the start and the end date, the Baseflow Index Method (BFI) from the "lfstat" package (Koffler et al., 2016) [33] in R was used. A detailed explanation of the BFI method can be found in the report on Low-flow Estimation and Prediction [34]. Hence, for each AM peak discharge value, the corresponding flood hydrograph was extracted from the daily discharge time series for all 107 stations.

3.2. Flood Typology

In order to analyze the compound flooding, the hydrographs were first divided into classes that included multivariate compound events and pre-conditioned compound events. The methodology used in this study is relatively similar to one implemented by Sikorska et al. (2015) [14], as some similar flood types were used. However, we decided to additionally distinguish between dry and wet event conditions (Table 3). This resulted in the eight flood types presented in Table 3.

Sikorska et al. (2015) [14] indicated that when snow cover exceeded 5% of the catchment area, the flood can be considered as influenced by snow, and the flood type in this case is either a snowmelt (SMF) flood or a rain-on-snow (ROS) flood. In case rain falls on top of the existing snow cover, then this is considered a ROS event. The threshold for precipitation used in this study to identify the ROS flood was 12 mm, which causes more than 1 mm of snowmelt (Table 3). The amount of snowmelt was determined by subtracting the snow thickness liquid water equivalent (LWE) from the previous day's LWE. The total thickness of the solid snow was not considered in this calculation because snow thickness can decrease, which changes the density of the snow without causing snowmelt runoff [35]. A SMF flood occurs when snowmelt exceeds 1 mm and less than 12 mm of precipitation falls (Table 3). To determine if the snow cover was in an initial wet or dry condition, snow density characteristics were investigated. Kuusisto (1984) [35] studied snow density during melting periods. Snow density depends on many factors, including snow thickness, air and snow temperature, precipitation, etc. Moreover, snow density can also vary regionally, and thus a direct comparison of snow densities between the selected catchments would not be an optimal solution. Therefore, the percentage of snow density increase during the melting phase can be compared. Kuusisto (1984) [35] wrote that snow density increased by more than 20% during the final phase of melting. This value (i.e., 20%) was used in the study as a threshold to determine whether the conditions were initially wet or dry. If snow density increased by more than 20% from the beginning of the hydrograph to the day of maximum snowmelt, it can be assumed that the snow was not in the process of melting, and the event (i.e., hydrograph) can be classified as an initial dry condition. If the increase in density was less than 20%, it can be assumed that the snow was already close to melting. Hence, the hydrograph can be classified as having initial wet conditions. Furthermore, the day of maximum snowmelt was used to determine the change in density, since there may be situations where, on the day of the peak hydrograph, the snow cover and thickness is close to zero, meaning that all the snow has already been melted. To obtain the snow density, the LWE was compared to the total solid snow thickness.

In cases when snow cover is less than 5% of the catchment area, it can be assumed that snowmelt has a minor impact on flood generation [14]. In this case, the main driver of the flood event is precipitation. The precipitation floods in the study were divided into short-precipitation floods (SPF) and long-precipitation floods (LPF). A SPF event occurs when the rainfall duration does not exceed 1 day and rainfall amount is greater than 12 mm. A LPF occurs when the rainfall duration is from 2 to 4 days and the rainfall amount exceeds 25 mm [14,36]. In the case that both conditions are fulfilled, the event was classified as LPF.

Moreover, multiple peaks in the hydrograph were assumed to be the LPF event [36]. The R package "pracma" was used to determine the number of peaks in the hydrograph [37].

Soil moisture data were used to determine the initial conditions (i.e., wet or dry) of the event. In order to calculate the percent saturation, data for each catchment were examined, and the largest daily volumetric water content for each catchment was defined. This maximum water content was assumed to be 100% saturation. All other values were then selected as numerators above this maximum value, resulting in the daily percent saturation content. The threshold was set at 75% (Table 3). This threshold was selected after some preliminary investigations and it was found to be a reasonable threshold to be used in relation to defining the antecedent conditions. By applying these constraints to each of the identified flood hydrographs, they were classified into eight categories. If an individual flood hydrograph did not meet any of the eight pre-determined categories (Table 3), it was classified in the "other" category. Figure 5 shows the classification process.

Table 3. Flood typology used in this study. References that were used to define the threshold values are presented in the square brackets.

Flood Type	Precipitation [14]	Snow Cover [14]	Snowmelt [14]	Antecedent Moisture Condition	Other [36]	Abbreviation
Rain-on-Snow Flood with Dry Conditions	>12 mm	>5%	>1 mm	>20% Increase in snow density [35]		ROS-D
Rain-on-Snow Flood with Wet Conditions	>12 mm	>5%	>1 mm	<20% Increase in snow density [35]		ROS-W
Snowmelt Flood with Dry Conditions	<12 mm	>5%	>1 mm	>20% Increase in snow density [35]		SMF-D
Snowmelt Flood with Wet Conditions	<12 mm	>5%	>1 mm	<20% Increase in snow density [35]		SMF-W
Long-Precipitation Floods with Dry Conditions	>25 mm over 4 days	<5%	<1 mm	<75% soil saturation at start of hydrograph	Multiple Peaks	LPF-D
Long-Precipitation Floods with Wet Conditions	>25 mm over 4 days	<5%	<1 mm	>75% soil saturation at start of hydrograph	Multiple Peaks	LPF-W
Short-Precipitation Floods with Dry Conditions	>12 mm in 1 day	<5%	<1 mm	<75% soil saturation at start of hydrograph		SPF-D
Short-Precipitation Floods with Wet Conditions	>12 mm in 1 day	<5%	<1 mm	>75% soil saturation at start of hydrograph		SPF-W

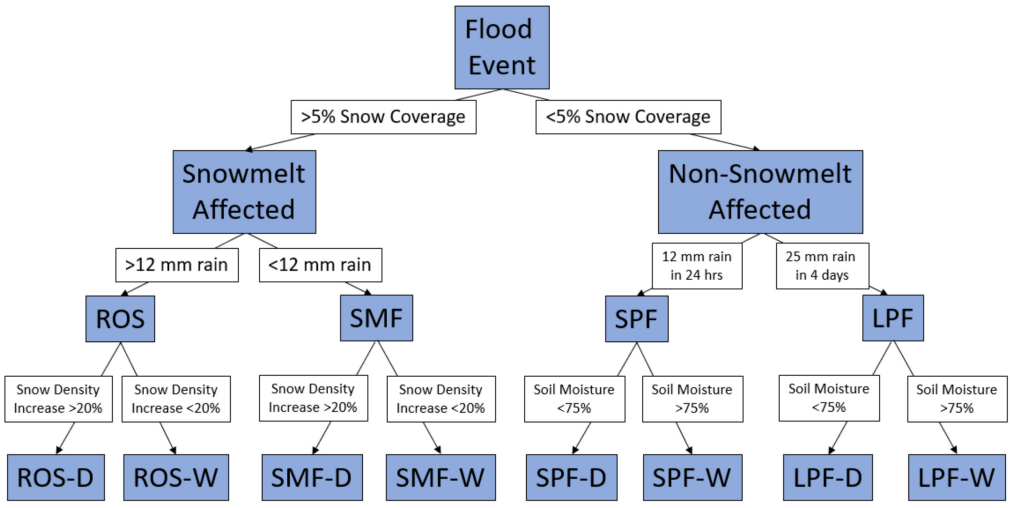

Figure 5. Visual representation of the flood classification process shown in Table 3.

Additionally, the differences in climate zones, catchment areas, and altitudes were also considered in analysis. The climate zone covering most of the catchment area was selected as the dominant zone of the individual catchment (see Supplement Figure S1). Four dominant climate zones were identified in the study, namely warm summer humid continental climate, temperate oceanic climate, tundra, and subarctic climate zone (see Supplement Figure S1). Other climate zones were only relevant to 1–3 catchments and were not considered in the classification by climate zone. The catchments were also divided into three categories according to their size (see Supplement Figure S2): large (>10,000 km^2), medium (between 200 and 10,000 km^2), and small (<200 km^2). Furthermore, the catchments were also divided into three categories by catchment mean elevation: high (>1000 m.a.s.l.), medium (between 500 and 1000 m.a.s.l.), and low (<500 m.a.s.l.) (see Supplement Figure S3).

4. Results and Discussion

4.1. Flood Typology Classification for All Catchments

Following the presented methodology for the extracted AM events (i.e., 41 events were extracted for each catchment), main climate characteristics during these events were examined (see Supplement Figures S4–S7). Some relatively large variability in the snow thickness, soil moisture and other variables during these events can be seen across Europe and North America (see Supplement Figures S4–S7). Hence, the percentage of snowmelt-related floods differed among the selected 107 catchments (see Supplement Figures S8 and S9). We argue that selected catchments represent a variety of conditions between the 40° and 70° latitude. Figures 6 and 7 show the results of the flood classification methodology for the selected European and North American catchments using heat maps. Several conclusions can be drawn from the heatmaps shown in Figures 6 and 7. Firstly, the majority of the AM floods that occurred in the investigated catchments (107 in total) were classified as snowmelt-driven floods (SMF). The snowmelt-driven floods (i.e., SMF-W and SMF-D types) represent 39% of all floods considered on both continents (Figures 6 and 7). Secondly, for all categories (i.e., ROS, SMF, SPF, and LPF), the wet conditions (-W) were always more prevalent than the dry conditions (-D) (Figures 6 and 7). The dry initial conditions accounted for 45%, 36%, 20%, and 19% of ROS, SMF, SPF, and LPF, respectively (Figures 6 and 7). These results are in accordance with what was reported in some previous studies that pointed to the importance of soil moisture on flood generation [16,38]. It should be noted that the percentage of dry initial conditions (-D) was higher for the snow-influenced floods (i.e., ROS and SMF) compared to SPF and LPF. Hence, high soil moisture values frequently occur with SPF and LPF events, and compound occurrence frequently results in flooding. It should be noted that the dry initial conditions for the snow-influenced floods were determined based on snow density. More specifically, the ROS floods made up 55% of the floods in the wet initial condition (Figures 6 and 7). The main reason for this is that rain quickly increases snow density prior to melting [39]. Furthermore, less than 20% of SPF and LPF events were seen where the maximum annual flood started at less than 75% soil saturation. Based on this fact, it is reasonable to assume that antecedent soil moisture is an important driver in flood generation in Europe and North America. These results are consistent with findings from previous studies [16,38]. It can also be seen that the percentage of SMF-W in general decreased from north to south (Figures 6 and 7). For flood hydrographs that we could not classify into any of the predefined categories for the North America catchments (i.e., Other type), an opposite situation is evident (Figure 6). For European catchments, the percentage of SPF-W and LPF-W generally increases from south to north (Figure 7). It should be noted that the selected thresholds (Table 3) could have an impact on the percentage of the occurrence of different flood types. For example, increasing the snow cover threshold (i.e., from 5% to 10 or 15%) would reduce the number of snow-related flood events. Additionally, increasing the 12 mm precipitation threshold related to the SPF events would decrease the number of these events. However, we argue that smaller changes in the selected thresholds would have a relatively minor impact on the presented results.

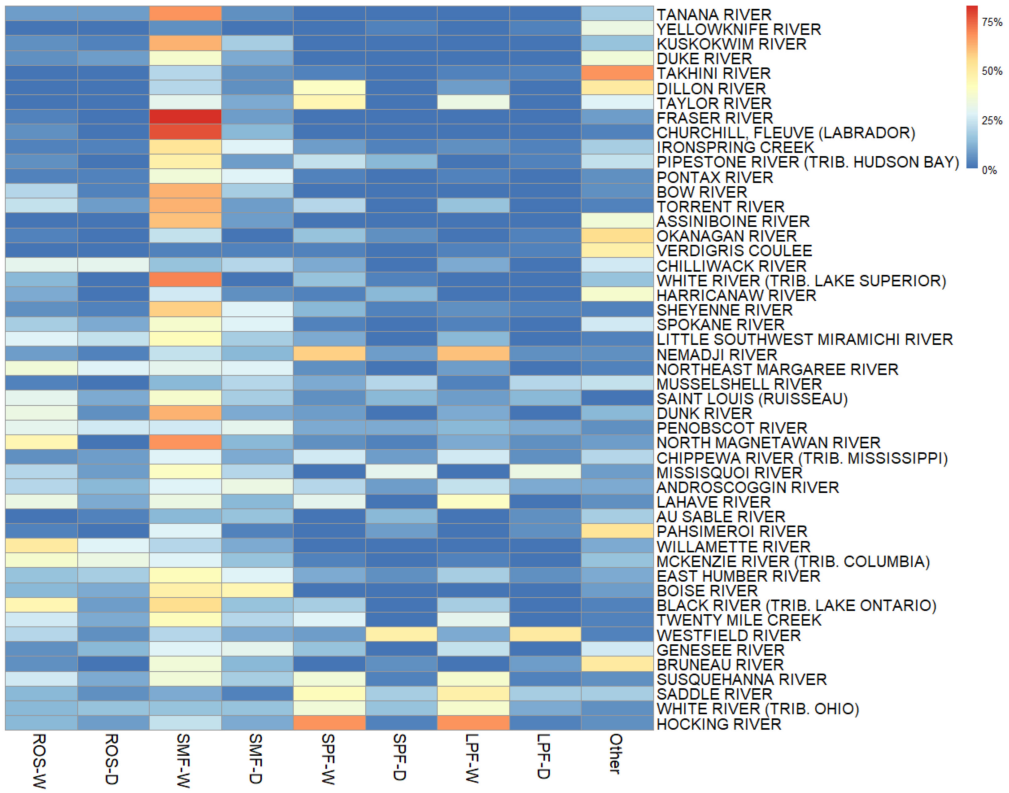

Figure 6. Heatmap for the North American catchment distribution of annual maximum (AM) flood typologies. Catchments are sorted from the south to the north.

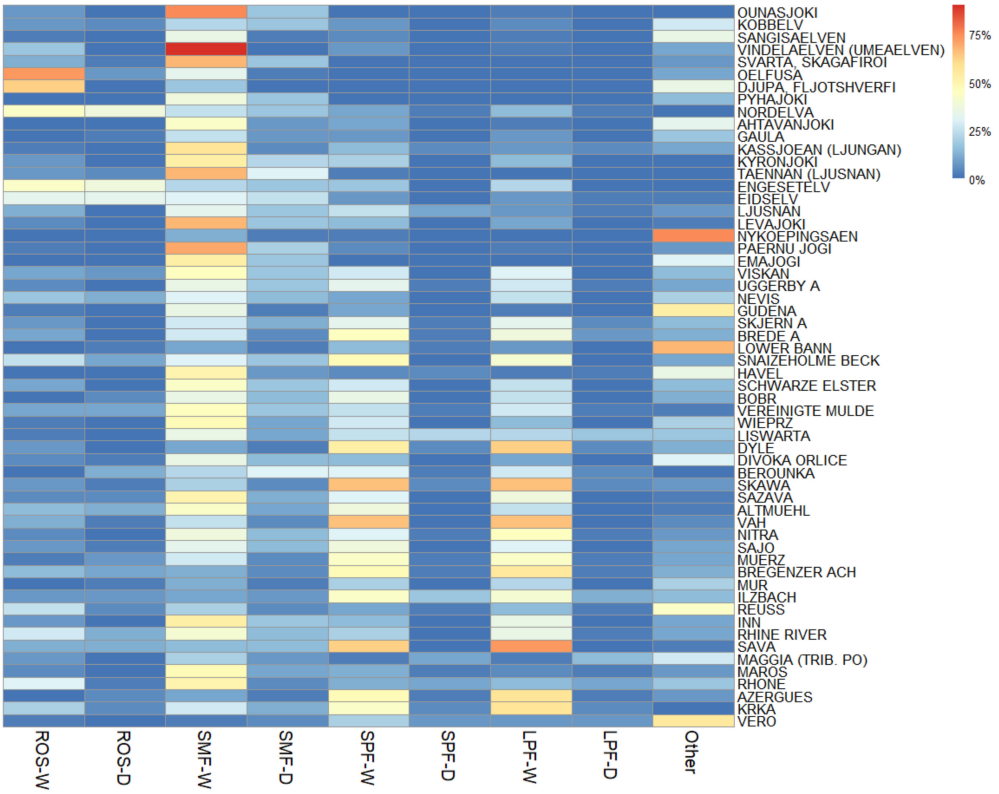

Figure 7. Heatmap for the European catchment distribution of annual maximum (AM) flood typologies. Catchments are sorted from south to north.

4.2. Flood Typology Classification Based on Climate Zone

The flood types were also classified based on the predefined climate zone of each catchment. For each climate zone, the mean distribution of flood typologies was considered. Figure 8 shows that the CFB and DFA zones are more evenly distributed across the different typologies, with the SPF and LPF being nearly equal to the SMF. The DFC zone has the highest magnitude of floods in the SMF-W category (Figure 8). The ET climate zone is dominated by the two dominant flood types, namely SMF-W and ROS-W (Figure 8). ET is the only one of the four climate zones (i.e., CFB, DFA, DFC, and ET) that includes more than three catchments, where ROS-W occured as the dominant flood type (Figure 8). This is likely due to the large amounts of rainfall in many mountainous regions where the ET climate is found [14].

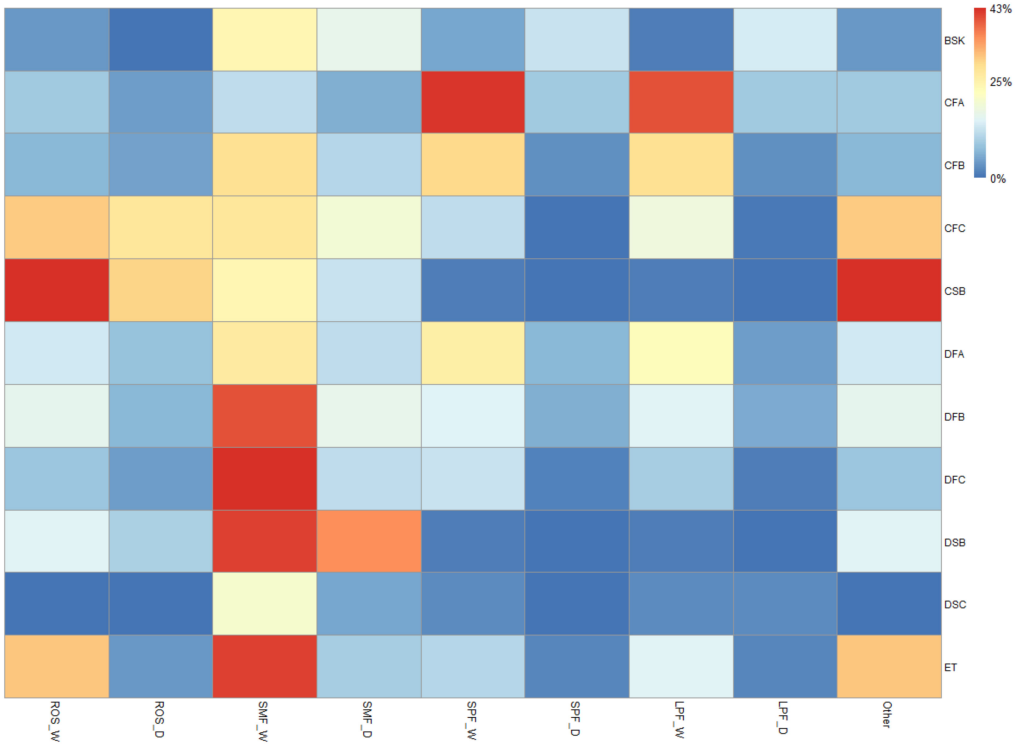

Figure 8. Heatmap for the annual maximum (AM) flood typology classification by climate zone, showing results for the four climate zones with the highest number of catchments.

4.3. Flood Typology Classification Based on Catchment Area

Figure 9 shows the flood types classified based on the size of the catchments. The SMF floods dominate in the large catchments, whereas the SPF and LPF are more common in the other two categories (Figure 9). There are several reasons for these results, one of which is the threshold related to the snow cover used to classify hydrographs (Table 3). The threshold for the snow cover, above which the flood was considered to be influenced by snow, was 5% (Table 3). In case of very large catchments, it is more likely that a part of the catchment is covered with snow, exceeding the threshold for a flood to be influenced by snowmelt. On the other hand, small catchments may be completely without snow coverage since small catchments do not cover large geographical areas. Additionally, several larger catchments in North America are located at higher latitudes. Another possible reason for these results is the soil moisture concept discussed by Harpold et al. (2015) [39]. Harpold et al. (2015) [39] argued that the highest soil moisture is reached within 5 days after the snowpack has completely melted. Moreover, in the case of large catchments, a rainfall storm would need to have a large spatial extent in order that catchment reaches the soil moisture required for an annual maxima flood generation. Hence, if a spatially extensive snowpack melts throughout the watershed, the entire watershed can reach the

high soil moisture required. The number of LPFs is relatively small for large catchments (Figure 9), which is to some extent an unexpected result, as LPFs generally have the ability to saturate large catchments, while on the other hand, the spatial extent of most extreme and short-duration precipitation events (i.e., SPFs) may be spatially limited [9]. Moreover, the results indicate that the medium and small catchments are dominated by SPFs and LPFs (Figure 9). This is likely due to the fact that the spatial extent of the storm required for these catchments to become saturated is generally smaller. Very extreme rainfall events (e.g., summer thunderstorms) tend to have a smaller spatial extent, which is why SPFs are more common in small- and medium-sized catchments (Figure 9) [15]. Additionally, small- and medium-sized catchments often have a shorter time of concentration compared to large catchments [15]. Thus, SPF and LPF can more easily saturate the entire small and medium catchments, resulting in high peak discharge values.

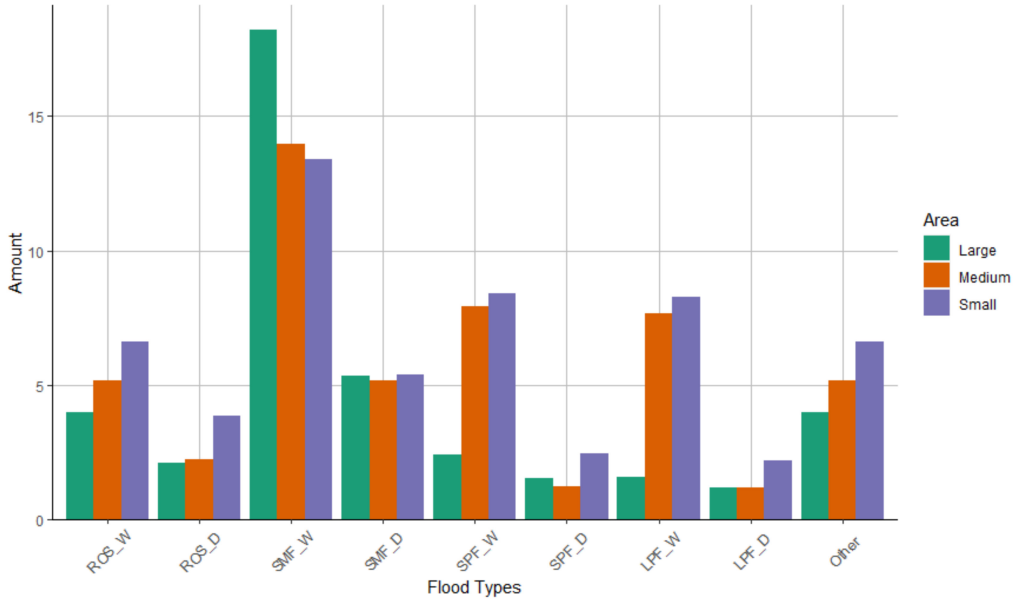

Figure 9. Flood typology classification based on the catchment area size.

4.4. Flood Typology Classification Based on Elevation

Figure 10 shows the distribution of floods in each flood type based on the mean elevation of the 107 catchments considered. It can be seen that the catchments at higher elevations have a slightly lower number of SMF and ROS floods than catchments at the medium and low elevations (Figure 10). A similar conclusion was also reached by Sikorska et al. (2015) [14]. Sikorska et al. (2015) [14] used two different methods to classify the floods. When investigating high-elevation catchments, they found that precipitation floods were the dominant flood type when using the crisp decision tree method [14], which is similar to the findings of this study (Figure 10). However, when they applied the fuzzy method, they found that although the dominant flood type remained the precipitation-driven flood, many of the floods were also classified as SMF or ROS floods [14]. However, the snow-related aspects do not exceed the thresholds to classify the flood as a snowmelt-affected flood. Sikorska et al. (2015) [14] hypothesized that this is due to a large amount of rainfall that falls in mountainous regions. Flash floods also often occur in mountainous catchments [14], which is not a flood type in the assessment shown in this study (Table 3). Moreover, Berghuijs et al. (2019) [16] found that extreme precipitation is the only predominant driver in mountainous regions [16]. Despite the large amounts of snow in the mountainous regions, rainfall can form the dominant flood type, which is caused by rainfall rather than snowmelt.

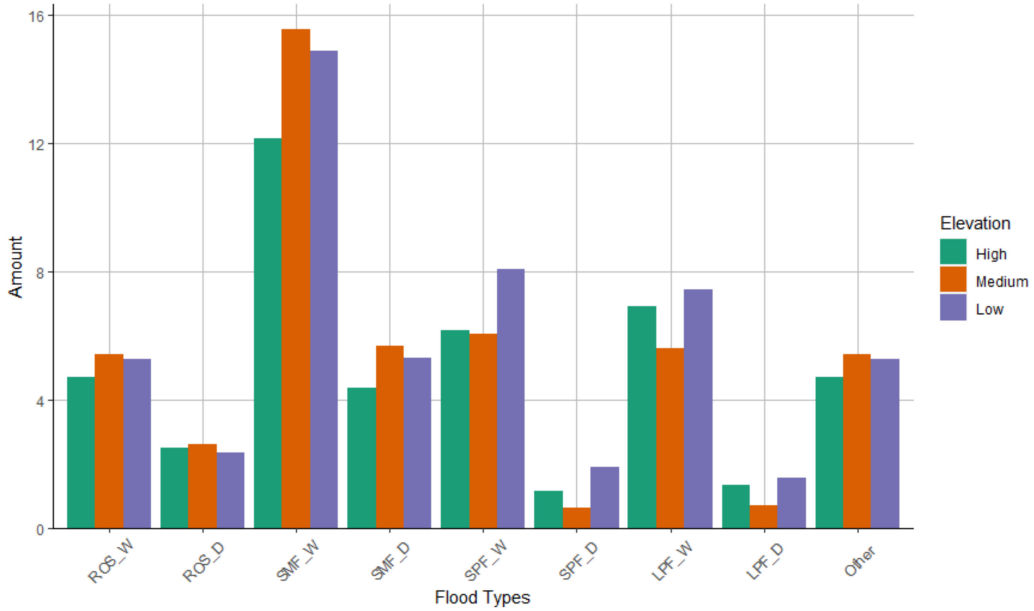

Figure 10. Flood typology classification based on the catchment elevation.

5. Conclusions

Based on the conducted analyses that were made based on the 107 selected catchments, several important conclusions can be made. It should be noted that the selection of 107 catchments that are relatively uniformly distributed between 40° and 70° latitude in Europe and North America represent a subset of all catchments and that different selection of catchments could yield different results. However, we argue that 107 catchments are representative for the selected study area. The results presented in this study indicate that snowmelt floods (especially SMF-W events) are often the dominant flood type in the catchments considered, especially for the catchments located at higher latitudes.

When comparing the relationships between the flood types (Table 3) and the climate zones, catchment elevation, and size, further conclusions could be made. Firstly, the primary flood type in the DFC and ET zones was SMF-W (Figure 8). Secondly, it was also shown that the large catchments had a slightly higher proportion of SMFs (Figure 9), while the medium and small catchments had slightly larger numbers of SPFs and LPFs (Figure 9). Thirdly, the occurrence of some specific flood types was found to change with latitude (e.g., SMF-W slightly decreased from south to north in Europe and North America). Finally, floods with wet soil initial condition (-W) occurred much more frequently than floods with the dry soil initial conditions (-D) in our analysis (Figures 6–10). The high frequency of the floods with wet soil initial conditions (-W) indicates that this may be a type of compound event—where a high antecedent moisture condition would qualify as a pre-existing event. In summary, these findings could be useful in the flood forecasting process, where special focus could be given to situations where soil moisture is high and a medium-precipitation event is expected in the following days. Additionally, these results could be used in the process of optimizing the flood risk management in relation to specific catchment characteristics (i.e., size, elevation, location climate). Moreover, finding could also be used for design of flood protection measures such as hybrid infrastructure. In the future, a similar study could be conducted, taking into account additional influencing factors (e.g., soil temperature as a proxy of ground frozenness) using an even larger number of catchments and testing different thresholds, which could be supplemented with additional statistical analysis.

Supplementary Materials: The following supporting information can be downloaded at: https://www.mdpi.com/article/10.3390/ijgi11120580/s1, Figure S1: Distribution of the selected 107 catchments per climate zone; Figure S2: Number of catchments based on the size of the catchment area. Small catchments have less than 200 km^2, large catchments are greater than 10,000 km^2 and medium catchments are between 200 and 10,000 km^2; Figure S3: Number of catchments based on the elevation. High elevation catchments are greater than 1000 m.a.s.l. Low elevation catchments are less than 500 m.a.s.l. Medium elevation catchments are between 500 and 1000 m.a.s.l; Figure S4: Mean snow thickness in the selected North American catchments during annual maximum events in the period 1979–2019; Figure S5: Mean snow thickness in the selected European catchments during annual maximum events in the period 1979–2019; Figure S6: Mean soil moisture in the selected North American catchments during annual maximum events in the period 1979–2019; Figure S7: Mean soil moisture in the selected European catchments during annual maximum events in the period 1979–2019; Figure S8: Percentage of annual maximum events that were affected by snowmelt in North America in the period 1979–2019; Figure S9: Percentage of annual maximum events that were affected by snowmelt in Europe in the period 1979–2019; Table S1: A list of 107 selected catchments with their main characteristics.

Author Contributions: Steven Brazda: methodology, investigation, formal analysis, data curation, writing—original draft; Mojca Šraj: writing—review and editing, conceptualization, supervision; Nejc Bezak: conceptualization, methodology, writing—review and editing, supervision. All authors have read and agreed to the published version of the manuscript.

Funding: The authors would like to acknowledge the support of the Slovenian Research Agency (ARRS) through grants P2-0180, V2-2137 and J6-4628 and support from the UNESCO Chair on Water-related Disaster Risk Reduction.

Data Availability Statement: Data can be obtained upon request.

Conflicts of Interest: The authors declare no conflict of interest.

References

1. Zscheischler, J.; Martius, O.; Westra, S.; Bevacqua, E.; Raymond, C.; Horton, R.M.; van den Hurk, B.; AghaKouchak, A.; Jézéquel, A.; Mahecha, M.D.; et al. A typology of compound weather and climate events. *Nat. Rev. Earth Environ.* **2020**, *1*, 333–347. [CrossRef]
2. Wachowicz, L.J.; Mote, T.L.; Henderson, G.R. A rain on snow climatology and temporal analysis for the eastern United States. *Phys. Geogr.* **2020**, *41*, 54–69. [CrossRef]
3. Sezen, C.; Šraj, M.; Medved, A.; Bezak, N. Investigation of rain-on-snow floods under climate change. *Appl. Sci.* **2020**, *10*, 1242. [CrossRef]
4. Sutanto, S.J.; Vitolo, C.; Di Napoli, C.; D'Andrea, M.; Van Lanen, H.A.J. Heatwaves, droughts, and fires: Exploring compound and cascading dry hazards at the pan-European scale. *Environ. Int.* **2020**, *134*, 105276. [CrossRef] [PubMed]
5. Bezak, N.; Mikoš, M. Changes in the compound drought and extreme heat occurrence in the 1961–2018 period at the european scale. *Water* **2020**, *12*, 3543. [CrossRef]
6. Mikoš, M.; Četina, M.; Brilly, M. Hydrologic conditions responsible for triggering the Stože landslide, Slovenia. *Eng. Geol.* **2004**, *73*, 193–213. [CrossRef]
7. Mikoš, M. After 2000 Stože landslide: Part II—Development in landslide disaster risk reduction policy in Slovenia—Po zemeljskem plazu Stože leta 2000: Del II—Razvoj politike zmanjševanja tveganja nesreč zaradi zemeljskih plazov v Sloveniji. *Acta Hydrotech.* **2021**, *34*, 39–59. [CrossRef]
8. Mikoš, M. After 2000 Stože landslide: Part I—Development in landslide research in Slovenia—Po zemeljskem plazu Stože leta 2000: Del I—Razvoj raziskovanja zemeljskih plazov v Sloveniji. *Acta Hydrotech.* **2020**, *33*, 129–153. [CrossRef]
9. Berghuijs, W.R.; Allen, S.T.; Harrigan, S.; Kirchner, J.W. Growing Spatial Scales of Synchronous River Flooding in Europe. *Geophys. Res. Lett.* **2019**, *46*, 1423–1428. [CrossRef]
10. Bezak, N.; Borrelli, P.; Panagos, P. A first assessment of rainfall erosivity synchrony scale at pan-European scale. *Catena* **2021**, *198*, 105060. [CrossRef]
11. Dietze, M.; Bell, R.; Ozturk, U.; Cook, K.L.; Andermann, C.; Beer, A.R.; Damm, B.; Lucia, A.; Fauer, F.S.; Nissen, K.M.; et al. More than heavy rain turning into fast-flowing water—A landscape perspective on the 2021 Eifel floods. *Nat. Hazards Earth Syst. Sci.* **2022**, *22*, 1845–1856. [CrossRef]
12. Brunner, M.I.; Viviroli, D.; Sikorska, A.E.; Vannier, O.; Favre, A.-C.; Seibert, J. Flood type specific construction of synthetic design hydrographs. *Water Resour. Res.* **2017**, *53*, 1390–1406. [CrossRef]
13. Poschlod, B.; Zscheischler, J.; Sillmann, J.; Wood, R.R.; Ludwig, R. Climate change effects on hydrometeorological compound events over southern Norway. *Weather Clim. Extrem.* **2020**, *28*, 100253. [CrossRef]

14. Sikorska, A.E.; Viviroli, D.; Seibert, J. Flood-type classification in mountainous catchments using crisp and fuzzy decision trees. *Water Resour. Res.* **2015**, *51*, 7959–7976. [CrossRef]
15. Merz, R.; Blöschl, G. A process typology of regional floods. *Water Resour. Res.* **2003**, *39*, 1–20. [CrossRef]
16. Berghuijs, W.R.; Harrigan, S.; Molnar, P.; Slater, L.J.; Kirchner, J.W. The Relative Importance of Different Flood-Generating Mechanisms Across Europe. *Water Resour. Res.* **2019**, *55*, 4582–4593. [CrossRef]
17. Brazda, S. *Snowmelt Floods in Relation to Compound Drivers in North Americ and Europe*; University of Ljubljana: Ljubljana, Slovenia, 2021.
18. GRDC. Global Runoff Data Centre (GRDC). Available online: https://www.bafg.de/GRDC/EN/Home/homepage_node.html (accessed on 1 March 2021).
19. CCID the Climate of the European ALPS: Shift of Very High Resolution Köppen-Geiger Climate Zones 1800–2100. Available online: http://koeppen-geiger.vu-wien.ac.at/alps.htm (accessed on 1 March 2021).
20. Amatulli, G.; Domisch, S.; Tuanmu, M.; Parmentier, B. Data Descriptor: A suite of global, cross-scale topographic variables for environmental and biodiversity modeling. *Sci. Data* **2018**, *5*, 180040. [CrossRef]
21. Copernicus Agrometeorological Indicators from 1979 to Present Derived from Reanalysis. Available online: https://cds.climate.copernicus.eu/cdsapp#!/dataset/10.24381/cds.6c68c9bb?tab=form (accessed on 15 March 2021).
22. Copernicus ERA5 Hourly Data on Single Levels from 1979 to Present. Available online: https://cds.climate.copernicus.eu/cdsapp#!/dataset/reanalysis-era5-single-levels?tab=overview (accessed on 20 March 2021).
23. Ozturk, U.; Saito, H.; Matsushi, Y.; Crisologo, I.; Schwanghart, W. Can global rainfall estimates (satellite and reanalysis) aid landslide hindcasting? *Landslides* **2021**, *18*, 3119–3133. [CrossRef]
24. Beck, H.E.; Pan, M.; Roy, T.; Weedon, G.P.; Pappenberger, F.; Van Dijk, A.I.J.M.; Huffman, G.J.; Adler, R.F.; Wood, E.F. Daily evaluation of 26 precipitation datasets using Stage-IV gauge-radar data for the CONUS. *Hydrol. Earth Syst. Sci.* **2019**, *23*, 207–224. [CrossRef]
25. Reder, A.; Rianna, G. Exploring ERA5 reanalysis potentialities for supporting landslide investigations: A test case from Campania Region (Southern Italy). *Landslides* **2021**, *18*, 1909–1924. [CrossRef]
26. R Core Team. *A Language and Environment for Statistical Computing*; R Foundation for Statistical Computing: Vienna, Austria, 2020.
27. Bezak, N.; Brilly, M.; Šraj, M. Comparison between the peaks-over-threshold method and the annual maximum method for flood frequency analysis | Comparaison entre les méthodes de dépassement de seuil et du maximum annuel pour les analyses de fréquence des crues. *Hydrol. Sci. J.* **2014**, *59*, 831174. [CrossRef]
28. Xiao, Y.; Guo, S.; Liu, P.; Yan, B.; Chen, L. Design flood hydrograph based on multicharacteristic synthesis index method. *J. Hydrol. Eng.* **2009**, *14*, 1359–1364. [CrossRef]
29. Bezak, N.; Horvat, A.; Šraj, M. Analysis of flood events in Slovenian streams. *J. Hydrol. Hydromech.* **2015**, *63*, 134–144. [CrossRef]
30. De Luca, P.; Hillier, J.K.; Wilby, R.L.; Quinn, N.W.; Harrigan, S. Extreme multi-basin flooding linked with extra-tropical cyclones. *Environ. Res. Lett.* **2017**, *12*, 114009. [CrossRef]
31. Eckhardt, K. How to construct recursive digital filters for baseflow separation. *Hydrol. Process.* **2005**, *19*, 507–515. [CrossRef]
32. Stoelzle, M.; Schuetz, T.; Weiler, M.; Stahl, K.; Tallaksen, L.M. Beyond binary baseflow separation: A delayed-flow index for multiple streamflow contributions. *Hydrol. Earth Syst. Sci.* **2020**, *24*, 849–867. [CrossRef]
33. Koffler, D.; Gauster, T.; Laaha, G. Package "Lfstat". 2016. Available online: https://cran.r-project.org/web/packages/lfstat/index.html (accessed on 15 September 2022).
34. Gustard, A.; Demuth, S. *Manual on Low-Flow Estimation and Prediction*; German National Committee for the International Hydrological Programme (IHP) of UNESCO and the Hydrology and Water Resources Programme (HWRP) of WMO Koblenz: Koblenz, Germany, 2009.
35. Kuusisto, E. *Snow Accumultation and Snowmelt in Finland*; National Board of Waters: Helsinki, Finland, 1984.
36. Fischer, S.; Schumann, A.; Bühler, P. Timescale-based flood typing to estimate temporal changes in flood frequencies. *Hydrol. Sci. J.* **2019**, *64*, 1867–1892. [CrossRef]
37. Borchers, H. Package "Pracma". 2021. Available online: https://cran.r-project.org/web/packages/pracma/index.html (accessed on 15 September 2022).
38. Blöschl, G.; Hall, J.; Viglione, A.; Perdigão, R.A.P.; Parajka, J.; Merz, B.; Lun, D.; Arheimer, B.; Aronica, G.T.; Bilibashi, A.; et al. Changing climate both increases and decreases European river floods. *Nature* **2019**, *573*, 108–111. [CrossRef]
39. Harpold, A.A.; Molotch, N.P.; Musselman, K.N.; Bales, R.C.; Kirchner, P.B.; Litvak, M.; Brooks, P.D. Soil moisture response to snowmelt timing in mixed-conifer subalpine forests. *Hydrol. Process.* **2015**, *29*, 2782–2798. [CrossRef]